ACS Photonics

Article

pubs.acs.org/journal/apchd5

Transparent and Flexible Polarization-Independent Microwave Broadband Absorber

Taehee Jang,[†] Hongseok Youn,[†] Young Jae Shin,[‡] and L. Jay Guo*[,†,‡]

[†]Department of Electrical Engineering and Computer Science, University of Michigan, Ann Arbor, Michigan 48109, United States
[‡]Macromolecular Science and Engineering, University of Michigan, Ann Arbor, Michigan 48109, United States

ABSTRACT: We present an optically transparent, flexible, and polarization-independent broadband microwave absorber. It is designed to possess two spectrally overlapped resonances of a bow-tie array, which originates from the fundamental resonance mode and the coupling between the neighboring units. An Al wire gird is used to construct the bow-tie array to induce high ohmic loss and broaden the bandwidth of the resonances. As a result, the combined resonances lead to more than 90% total absorption covering a wide frequency range from 5.8 to 12.2 GHz. The transparent and flexible properties provide more flexibility for absorber applications. The optical transmittance of the whole structure is more than 62%.

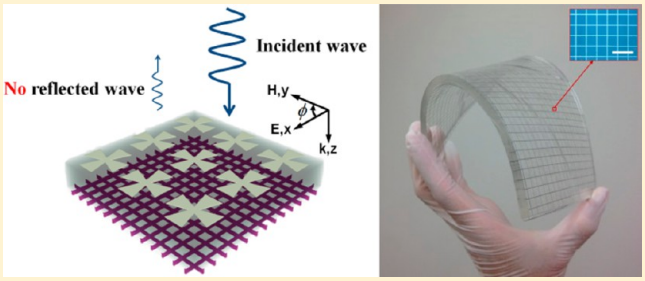

KEYWORDS: *transparent, flexible, broadband, microwave, absorber*

Broadband absorbers can reduce the reflection and scattering of electromagnetic (EM) waves from the structures over a wide frequency range. They can be exploited to enhance the efficiency of photovoltaic devices[1,2] and thermal detectors[3] and can also render objects undetectable by EM waves.[4] Absorbers can be designed by using classical electromagnetic wave theory or by engineered metamaterials. Metamaterial absorbers have been designed by manipulating the effective permittivity $\varepsilon(\omega)$ and permeability $\mu(\omega)$ to match the impedance to free space.[5−9] The transmitted power is then absorbed by the structure due to the lossy components of permittivity and permeability. Although metamaterial-based absorbers offer the potential advantages of perfect absorption and thinness, it is difficult to utilize them for practical applications due to their very narrow bandwidths. In order to improve the bandwidth, multiband absorbers have been introduced that utilize multiple layered structures.[10,11] However, not only are these multilayered structures thick but also they require a complicated fabrication process. Classical electromagnetic absorbers can be realized by placing one or more additional resistive sheets in the structure in order to generate losses to the incident field. A Salisbury screen is one of the classic electromagnetic absorbers that have a resistive sheet placed at $\lambda/4$ over a ground plane.[12] This absorber has some drawbacks such as narrow bandwidth and relatively large thickness. Another classical absorber is the Jaumann absorber, which utilizes a multilayer structure to increase the bandwidth.[13,14] However, to obtain a broad bandwidth, the structure becomes very thick and bulky. In addition, the absorbers constructed from the conventional materials are typically rigid and optically opaque. If the absorber can be made optically transparent and structurally flexible, it can provide high design freedom for practical applications.[15,16] For example, an optically transparent and flexible absorber can be applied to applications such as window glass and curved surfaces.

In this paper, we propose and demonstrate an optically transparent, flexible, polarization-independent, and broadband microwave absorber. The absorber is based on two principles: (1) it utilizes resonant structure to provide the impedance match to the air, such that EM energy can be coupled into the structure with little reflection; (2) the resonator is made of an Al wire grid to induce ohmic loss and effectively dissipates the coupled EM energy to heat. We found that a bow-tie-shaped resonator provides easy tunability of the resonance bandwidth. The new structure is designed to possess two resonances resulting from symmetric bow-tie structures as well as the coupling between the neighboring bow-tie structures. Therefore the bow-tie array collectively provides a broadband response. The symmetric bow-tie structure also provides a polarization-independent property. The proposed structure is realized using an Al wire grid, a transparent and flexible polyethylene terephtalate (PET) film, and polydimethylsiloxane (PDMS) layers. The overall structure is transparent and flexible, which makes it possible to apply to curved surfaces. The fabricated absorber structure produces an absorption above 90% in the frequency range 5.8−12.2 GHz, and the bandwidth is 71.1% of the center frequency.

BROADBAND ABSORBER

Theoretical Consideration. In order to achieve the perfect absorption, the impedance of the absorber is matched to the air

Received: December 26, 2013
Published: February 19, 2014

and the transmitted waves are dissipated due to the loss components of the structure. The previously reported experiment of concealing an object by a carbon nanotube (CNT) coating across the entire visible band follows the same principle,[17] where the aligned CNTs with low fill ratio provided the index/impedance match to air and also absorb the light energy coupled into the CNT layer. However, to extend the approach to the microwave range, the required CNT thickness would be impractically thick. Instead we will use an array of resonant structures to achieve the impedance matching function. Figure 1a shows the structure for achieving broadband absorption. The total impedance of the structure is obtained from the combination of the impedances of a metallic resonator and a dielectric layer with the ground plane. The effective impedance of the structure can be obtained from[5]

$$Z_{\text{eff}}(\omega) = \sqrt{\frac{\mu_{\text{eff}}(\omega)}{\epsilon_{\text{eff}}(\omega)}} = \sqrt{\frac{(1+S_{11})^2 - S_{21}^2}{(1-S_{11})^2 - S_{21}^2}} \quad (1)$$

where $\epsilon_{\text{eff}}(\omega)$ and $\mu_{\text{eff}}(\omega)$ are the effective permittivity and permeability, respectively. The real and imaginary part of the impedance are calculated from the simulated complex S-parameters and plotted in Figure 2b. The effective impedance

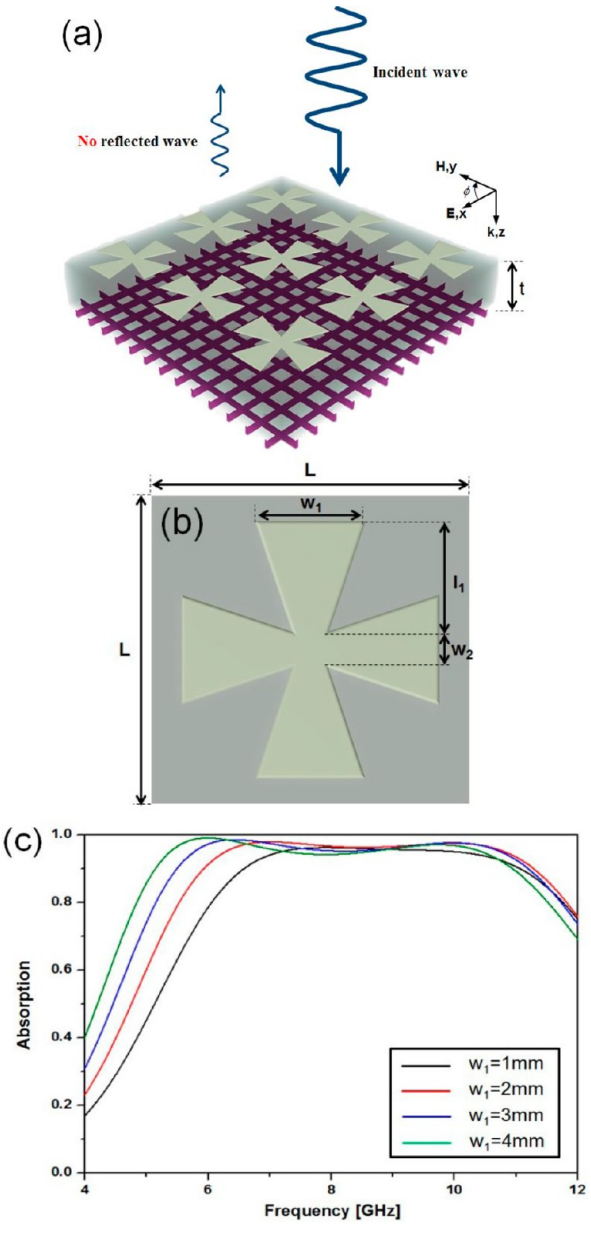

Figure 1. Schematic of broadband absorber: (a) perspective view and (b) top view (design parameters: w_1 = 4 mm, w_2 = 1 mm, l_1 = 4.2 mm, l = 10 mm). (c) Simulated absorption at different widths of the bow tie (w_1) (the 90% absorption bandwidth at w_1 = 1 mm: 50.4%, at w_1 = 2 mm: 61.6%, at w_1 = 3 mm: 68.2%, at w_1 = 4 mm: 72%) The inset shows the equivalent circuit model of the proposed absorber according to the frequency.

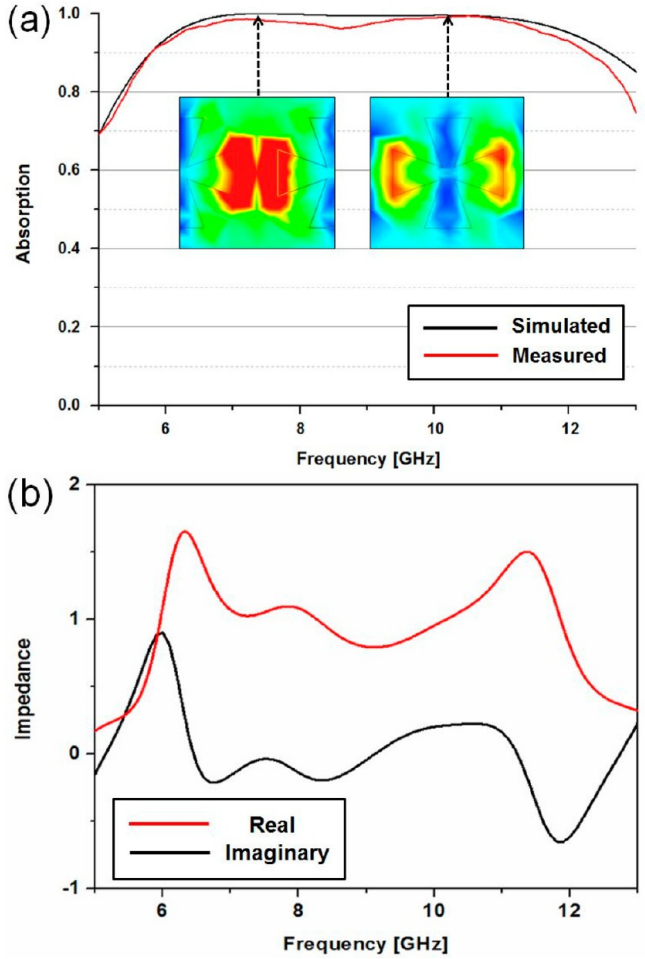

Figure 2. (a) Simulated and measured absorption according to the frequency. (b) Calculated real and imaginary part of the impedance.

of the structure has two matched bands by the change of the electric and magnetic response corresponding to the change of permittivity and permeability. Thus, the reflected wave is minimized.

The resonant structure having a high Q factor can be utilized in applications such as narrow band filters and oscillators that require high selectivity and low loss. To achieve broadband absorption, the Q factor of the structure should be reduced. This can be achieved by increasing the resistance, and the increased resistance also has the additional benefit of dissipating the energy, therefore resulting in minimized reflection over a broad frequency range. To increase the resistance, a bow-tie pattern of an Al wire grid is used to construct the resonant structure. For our design, we used a bow-tie-shaped resonator due to its symmetric configuration, which is less sensitive to the

dx.doi.org/10.1021/ph400172u | ACS Photonics 2014, 1, 279−284

polarization of the incident wave. More importantly, we will show that the bow-tie shape can offer a broader response range by exploiting not only its own resonance but also the coupling between the neighboring unit cells in a periodic array via the side of the bow ties. Regardless of the number of unit cells, the resonant frequency of the cascaded circuit is determined by the resonant frequency originating from the two kinds of equivalent circuit. By merging the two resonances, we achieved a broad bandwidth of 71.1% of the center frequency.

Realization of the Transparent and Flexible Structure. The proposed absorber is composed of top Al wire grid metallic patterned patches, PET, PDMS, and a metallic wire grid ground. Figure 1 shows the schematic of the proposed absorber consisting of an array of Al wire grid metallic bow-tie resonators on a PDMS dielectric layer backed by a metallic wire grid mesh ground plane. Figure 1a shows the proposed absorber arranged in a periodic array, and Figure 1b shows the unit cell with the design parameters. A flexible and transparent PET and PDMS layer separate the two metallic layers. Such flexible polymer layers with patterned bow-tie structures are optically transparent and can be applied to any metallic surface to provide the broadband absorption property.

In designing the broadband absorber, the geometric parameters, including the thickness of metallic patterns, are chosen to obtain the desired wave absorptions at two resonance frequencies, and these parameters are further optimized so that the two resonances are spectrally merged together to provide broadband characteristics. As an example, Figure 1c shows that as the base (w_1) of the bow tie increases, the absorption band extends to lower frequency range. Here, the length of the bow tie and the spacing are fixed to l = 10 mm and t = 5 mm, respectively. To reduce the reflection from the absorber structure, good impedance matching to air is required. This can be achieved by varying the spacing between bow-tie structure and dielectric spacer layer thickness as well as using the optimized metal thickness. In order to obtain greater than 90% absorption over the desired bands, the absorption magnitudes and frequencies at the two resonances are optimized by adjusting the thicknesses of the dielectric layer (PDMS) and the surface impedance of the metallic wire grid bow-tie resonator (aluminum). For the bow-tie-shaped resonator made of Al mesh with a surface resistance of 30 Ω/sq, the optimized Al thickness is 62 nm, while the PDMS layer with dielectric constant 2.25 and thickness 4.9 mm is utilized for a spacer. The surface resistivity of the deposited metal film was measured using a standard four-point probe configuration. Furthermore, a transparent metal mesh ground plane that provides optical transparency greater than 90%[18] is employed.

The RF reflectance and the transmittance are measured at normal incidence. The measured reflectance is normalized with respect to a metal plane with the same dimensions, while the measured transmittance is normalized with respect to the incident wave in free space. The measured transmission and reflection are then used to obtain the absorption, which is defined as $A(\omega) = 1 - T(\omega) - R(\omega)$, where $R(\omega) = |S_{11}|^2$ and $T(\omega) = |S_{21}|^2$ are the reflectance and transmittance obtained from the measured frequency-dependent complex S-parameter, respectively. In principle, when the impedance of the structure is matched to the air to minimize the reflection, a perfect absorption can be achieved because the metallic ground plane forbids any transmission through the structure. The simulated and measured $A(\omega)$ are plotted in Figure 2. As expected, transmission represented by $S_{21}(\omega)$ is nearly zero in the entire operating frequency range. To fabricate the absorber structure having an area of 300 mm × 200 mm, a 62-nm-thick aluminum layer was first deposited on a 50-μm-thick PET film by sputtering. The aluminum wire grid mesh was then patterned in the shape of a bow tie by optical lithography and etching. Then the PET film with patterned Al structure was attached to a thicker and more flexible PDMS layer. A picture of the fabricated bow-tie array on top of PET is shown in Figure 3a.

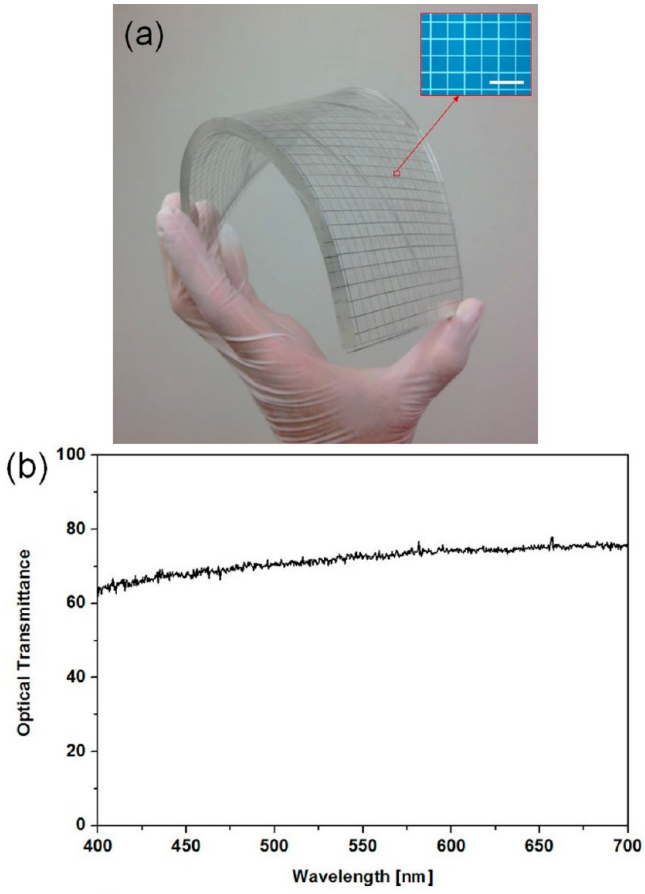

Figure 3. (a) Fabricated metallic bow-tie array on top of a flexible and transparent PET layer (scale bar = 100um). (b) Optical transmittance.

The inset in Figure 3a shows the zoomed view of the bow tie of the Al wire grid mesh. The fabricated structure is optically transparent and, when attached to a wire grid metallic ground plane, forms a complete absorber structure. The absorber was measured by using an HP 8720B network analyzer that covers the range 0.13−20 GHz and two broadband horn antennas in a microwave anechoic chamber. The wire grid mesh ground plane can act as the metal plane at the microwaves. The fabricated structure shows absorption greater than 90% in the frequency range 5.8−12.2 GHz, and the bandwidth is 71.1% of the center frequency. Figure 4 shows the measured absorptions for different polarizations of the incident wave. The optical transmittance of the total structure is more than 62%, as shown in Figure 3b.

Dependence of Polarization. Due to the symmetric pattern of the bow-tie structure, the absorption is almost polarization-independent. The polarization angle (ϕ) is defined as the angle between the electric field and x-axis. Figure 4 shows the measured absorption according to the polarization.

dx.doi.org/10.1021/ph400172u | ACS Photonics 2014, 1, 279−284

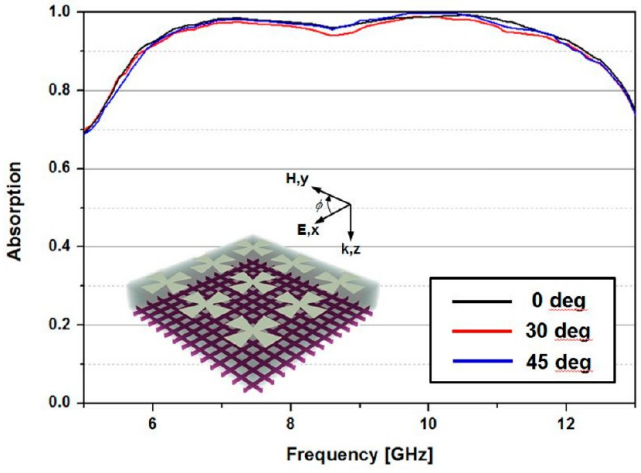

Figure 4. Measured absorptions at different polarization angle ϕ (0, 30, and 45 deg).

As ϕ increases, the absorption magnitudes and resonance frequencies of the absorber are nearly unchanged for different polarizations (0, 30, 45 deg) of the normal incident wave, demonstrating polarization-independence of the absorber structure.

Double Resonances. As can be seen in Figure 2a, there are two absorption peaks; the low-frequency resonance is mainly due to the coupling field between bow-tie structures, and the high frequency resonance is due to the fundamental resonant mode of the bow-tie structure as discussed below. To understand the origin of these two absorption peaks, the electrical field distribution and power flow are simulated and analyzed by using Ansoft high frequency structure simulator (HFSS) software. In the simulations, the top metallic wire grid bow-tie resonators are modeled as an impedance sheet with a sheet resistance of 30 Ω/sq, and the dielectric constant and loss tangent of the dielectric spacer are 2.25 and 0.01, respectively. A unit cell of the structure is simulated using periodic boundary conditions along the x and y directions. For the proposed absorber with w_1 = 4 mm, the absorber possesses two resonances, one at 7.4 GHz and the other at 10.1 GHz. In addition, as can be seen in Figure 2b, the calculated real and imaginary part of the impedance are almost unity and nearly zero between 7.4 and 10.1 GHz, respectively. Therefore impedance matching with air was achieved, which minimizes the reflection from the absorber. Figure 5a and b show the top view of the simulated electrical field distribution of the absorber structure at the two absorption peak frequencies (f_1 = 7.4 GHz and f_2 = 10.1 GHz), while Figure 5c and d show the simulated electrical field distribution at the central cross section. The electric fields are strongly localized in the gap between the two bow-tie structures at the low resonant frequency and are localized around the edges of the bow-tie structure at high resonant frequency. Figure 5e and f show the power flow of the absorber at two absorption peak frequencies. Figure 6a and b show the schematic of the electrical fields and power flows localized at low and high resonant frequencies, respectively. The behavior is similar to that of magnetostatic interference[19] in metallic slit structures, where the polarized electric charge produces a strong localized E-field, which guides the Poynting energy flow, as shown in Figure 6a and b. At low resonant frequency, most incident power flows through the gap between the bow-tie structures, while at high resonant frequency the power flow is toward the center of the bow-tie resonator. In both cases, the energy flowing into the bow tie was eventually dissipated due to the high ohmic loss of the Al wire grid that is

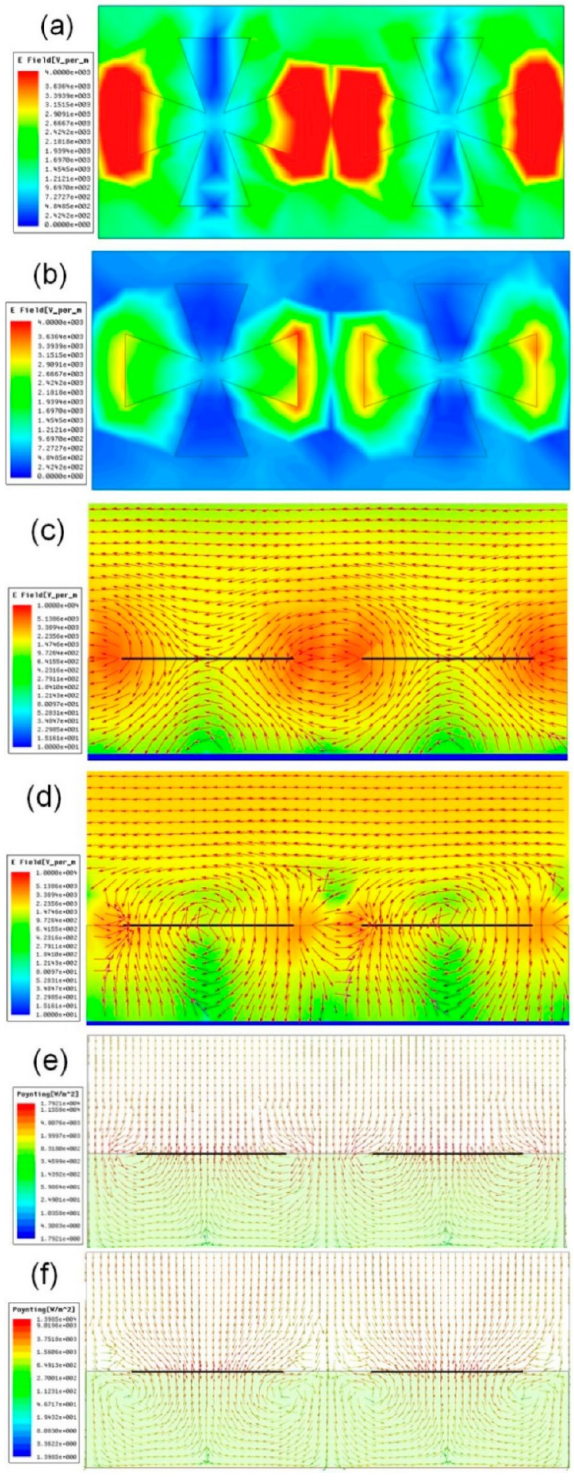

Figure 5. (a, b) Electrical amplitude in the top view at 7.4 and 10.1 GHz, respectively, and power flow at 7.4 and 10.1 GHz. (c, d) The colors represent the amplitude of the electric field and the arrows represent the direction of the electric field in the central cross section of the unit cell at 7.4 and 10.1 GHz, respectively. (e, f) The colors represent the amplitude of the power flow and the arrows represent the direction of the power flow in the central cross section of the unit cell at 7.4 and 10.1 GHz, respectively.

dx.doi.org/10.1021/ph400172u | ACS Photonics 2014, 1, 279−284

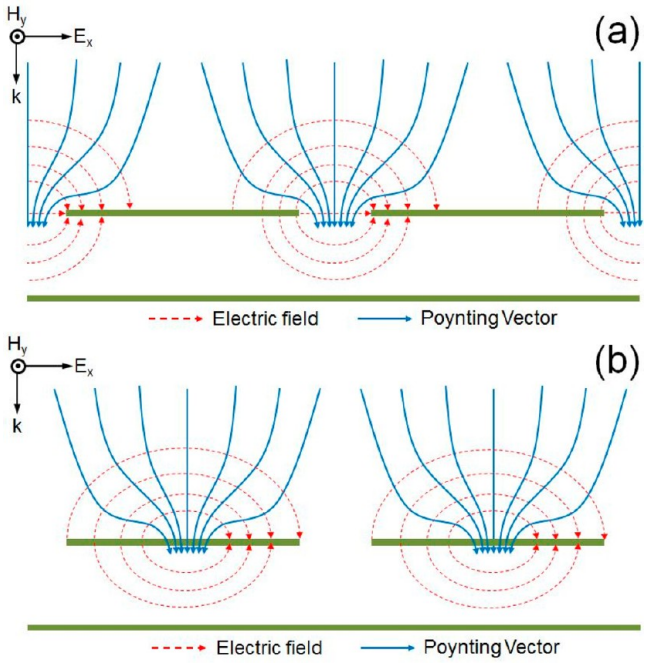

Figure 6. (a) Schematic of electric field and Poynting vector localized in the gap between the two bow-tie structures at the low resonant frequency. (b) Schematic of electric field and pointing vector localized around the edges of the bow-tie structure at high resonant frequency.

used to form the bow-tie structure. The above results verify that the two absorption peaks are contributed by the fundamental resonance of the bow-tie structure and the coupling between bow-tie structures, respectively. The merging of the two resonances with overlap spectra ensures the broadband performance of the proposed absorber.

CONCLUSION

Since the two absorption peaks are the result of energy flow and loss in different positions of the absorber, these can be adjusted by changing the width and length of the bow-tie structure respectively. For example, in Figure 1c, as the width of the bow tie increases from 1 mm to 4 mm, the absorption peak at low frequency is shifted to the lower frequency range due to the increased coupling between the neighboring bow-tie structures. Thus, the bandwidth to achieve more than 90% absorption can be extended by increasing the w_1. The spectral overlap of the two selected absorption bands broadens the absorption bandwidth. In addition, owing to simple periodically symmetric patterned structures, the absorber is independent of the polarizations of the incident wave.

Finally we discuss methods to further increase the absorption bandwidth. On the basis of the principle discussed above, even greater bandwidth can be obtained by merging multiple resonances with overlapped spectra. In order to achieve new resonances, bow-tie resonators having different geometric parameters can be inserted in the dielectric spacer as intermediate layers. Each layer generates two resonant frequencies by a similar principle. By adding the patterned structures having different lengths at thicknesses of t_1, $t_1 + t_2$, and $t_1 + t_2 + t_3$, respectively, different resonances can be obtained to increase the bandwidth. For example, a three-layer absorber is designed as shown in Figure 7a. We avoided the alignment of the patterned bow-tie structures in each layer as

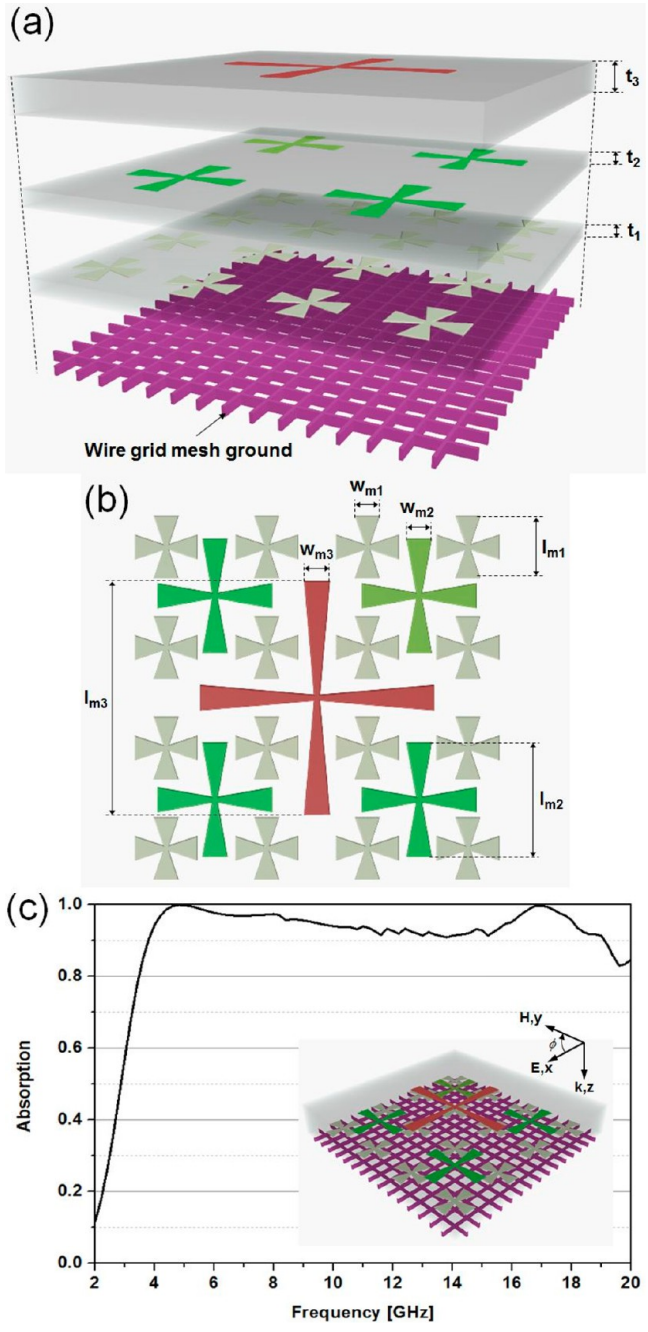

Figure 7. Configuration of the multilayer absorber structure: (a) perspective view; (b) top view; (c) simulated absorption (w_{m1} = 1.6 mm, w_{m2} = 2.2 mm, w_{m3} = 2.8 mm, l_{m1} = 5.1 mm, l_{m2} = 10.8 mm, l_{m3} = 19.4 mm, t_1 = 2.4 mm, t_2 = 2.2 mm, and t_3 = 4 mm).

shown in Figure 7b, so that the resonant fields are less affected by the presence of the neighboring layers. In the simulation, the bow-tie resonators in the first, second, and third layers from the ground plane are modeled with sheet resistances of 20, 20, and 25 Ω/sq respectively. Since the absorption peaks are located close to each other, the frequency range to achieve absorption above 90% is 3.8−19.2 GHz, and, therefore, the bandwidth of the three-layer absorber is enhanced to 133.9% of the center frequency as shown in Figure 7c.

The metal mesh structure used in our structure not only provides optical transparency but also increases the resistance, which is needed for the broadband application. The recently

dx.doi.org/10.1021/ph400172u | ACS Photonics 2014, 1, 279−284

developed photo roll lithography can be used to create a large area of such flexible absorbers in a roll-to-roll platform,[18,20] facilitating practical applications. With further development, we anticipate numerous applications of such transparent and broadband absorbers in the future, *e.g.*, zero-reflected power over a wide bandwidth for better aircraft stealth performance.

AUTHOR INFORMATION

Corresponding Author

*E-mail: guo@umich.edu.

Notes

The authors declare no competing financial interest.

ACKNOWLEDGMENTS

This work was supported in part by the AFOSR and NSF.

REFERENCES

(1) Aydin, K.; Ferry, V. E.; Briggs, R. M.; Atwater, H. A. Broadband Polarization-Independent Resonant Light Absorption Using Ultrathin Plasmonic Super Absorbers. *Nat. Commun.* **2011**, *2*, 517.

(2) Atwater, H. A.; Polman, A. Plasmonics for Improved Photovoltaic Devices. *Nat. Mater.* **2010**, *9*, 205−213.

(3) Zhu, H.; Yi, F.; Cubukcu, E. Nanoantenna Absorber for Thermal Detectors. *Photon. Tech. Lett., IEEE* **2012**, *24*, 1194−1196.

(4) Emerson, W. Electromagnetic Wave Absorbers and Anechoic Chambers through the Years. *IEEE Trans. Antennas Propagation* **1973**, *21*, 484−490.

(5) Smith, D. R.; Vier, D. C.; Koschny, T.; Soukoulis, C. M. Electromagnetic Parameter Retrieval from Inhomogeneous Metamaterials. *Phys. Rev. E* **2005**, *71*, 036617.

(6) Landy, N. I.; Sajuyigbe, S.; Mock, J. J.; Smith, D. R.; Padilla, W. J. Perfect Metamaterial Absorber. *Phys. Rev. Lett.* **2008**, *100*, 207402.

(7) Tao, H.; Landy, N. I.; Bingham, C. M.; Zhang, X.; Averitt, R. D.; Padilla, W. J. A Metamaterial Absorber for the Terahertz Regime: Design, Fabrication and Characterization. *Opt. Express* **2008**, *16*, 7181−7188.

(8) Bhattacharyya, S.; Ghosh, S.; Srivastava, K. V. Triple Band Polarization-Independent Metamaterial Absorber with Bandwidth Enhancement at X-band. *J. Appl. Phys.* **2013**, *114*, 094514.

(9) Dincer, F.; Karaaslan, M.; Unal, E.; Sabah, C. Dual-Band Polarization Independent Metamaterial Absorber Based on Omega Resonator and Octa-Starstrip Configuration. *Prog. Electromagn. Res.* **2013**, *141*, 219−231.

(10) Grant, J.; Ma, Y.; Saha, S.; Khalid, A.; Cumming, D. R. S. Polarization Insensitive, Broadband Terahertz Metamaterial Absorber. *Opt. Lett.* **2011**, *36*, 3476−3478.

(11) Ye, Y. Q.; Jin, Y.; He, S. Omnidirectional, Polarization-Insensitive and Broadband Thin Absorber in the Terahertz Regime. *J. Opt. Soc. Am. B* **2010**, *27*, 498−504.

(12) Salisbury, W. W. U.S. Patent 2599944, 1952.

(13) Ruck, G. T.; Barrick, D. E.; Stuart, W. D. *Radar Cross Section Handbook*, Vol. 2; Plenum: New York, 1970.

(14) Knott, E.; Shaeffer, J. F.; Tuley, M. T. *Radar Cross Section*, 2nd ed.; Scitech: Raleigh, 2004.

(15) Okano, Y.; Ogino, S.; Ishikawa, K. Development of Optically Transparent Ultrathin Microwave Absorber for Ultrahigh-Frequency RF Identification System. *IEEE Trans. Microwave Theor. Tech.* **2012**, *60*, 2456−2464.

(16) Singh, P. K.; Korolev, K. A.; Afsar, M. N.; Sonkusale, S. Single and Dual Band 77/95/110 GHz Metamaterial Absorbers on Flexible Polymide Substrate. *Appl. Phys. Lett.* **2011**, *99*, 264101.

(17) Shi, H.; Ok, J. G.; Baac, H. W.; Guo, L. J. Low Density Carbon Nanotube Forest as an Index-Matched and near Perfect Absorption Coating. *Appl. Phys. Lett.* **2011**, *99*, 211103.

(18) Kwak, M. K.; Ok, J. G.; Lee, J. Y.; Guo, L. J. Continuous Phase-Shift Lithography with a Roll-Type Mask and Application to Transparent Conductor Fabrication. *Nanotechnology* **2012**, *23*, 344008.

(19) Pardo, F.; Bouchon, P.; Haidar, R.; Pelouard, J.-L. Light Funneling Mechanism Explained by Magnetoelectric Interference. *Phys. Rev. Lett.* **2011**, *107*, 093902.

(20) Ok, J. G.; Kwak, M. K.; Huard, C. M.; Guo, L. J. Photo-Roll Lithography (PRL) for Continuous and Scalable Patterning with Application in Flexible Electronics. *Adv. Mater.* **2013**, *25*, 6554−6561.